

Rovibrational Overtone and Combination Bands of the HCNH^+ Ion

Miroslava Kassayová^a, Miguel Jiménez-Redondo^b, János Sarka^{c,d}, Petr Dohnal^a, Juraj Glosík^a, Paola Caselli^b and Pavol Jusko^{b,*}

^aDepartment of Surface and Plasma Science, Faculty of Mathematics and Physics, Charles University, V Holešovičkách 2, Prague, 18000, Czech republic

^bMax Planck Institute for Extraterrestrial Physics, Gießenbachstraße 1, Garching, 85748, Germany

^cI. Physikalisches Institut, Universität zu Köln, Zùlpicher Str. 77, Cologne, 50937, Germany

^dInstitute of Chemistry, Eötvös Loránd University, Pázmány Péter sétány 1/A., Budapest, 1117, Hungary

ARTICLE INFO

Keywords:

HCNH^+

rovibrational spectroscopy

overtone/ combination bands

action spectroscopy

cryogenic ion trap

active background suppression

ABSTRACT

Spectra of vibrational overtone and combination bands from vibrational ground state of HCNH^+ were measured using an action spectroscopy technique with active background suppression in a cryogenic 22 pole radio frequency ion trap apparatus. Spectroscopic constants for the upper vibrational levels of the transitions were determined with vibrational band origins being $6846.77981(90) \text{ cm}^{-1}$ ($2\nu_1$, NH stretch), $6640.47624(43) \text{ cm}^{-1}$ ($\nu_1 + \nu_2$), $6282.03578(63) \text{ cm}^{-1}$ ($2\nu_2$, CH stretch), and $6588.4894(20) \text{ cm}^{-1}$ ($\nu_2 + \nu_3 + 2\nu_5^0$). State of the art *ab initio* VCI calculations up to 10^4 cm^{-1} complement the experimental data.

1. Introduction

The gas-phase ion-molecule chemistry of both diffuse and dense interstellar clouds has been extensively investigated over the years, contributing to our understanding of the interstellar medium (ISM) and its complex chemical processes [1]. Among the key molecular ions studied is HCNH^+ , a linear, closed-shell species that plays a significant role in interstellar chemistry [2, 3, 4, 5]. HCNH^+ is considered to be the primary precursor for the formation of HCN and HNC [6, 3, 4], both of which are crucial molecules in the ISM [7]. In particular, HCN is considered an essential precursor of prebiotic molecules, including sugars, nucleotides, amino acids, and fatty acids (e.g. [8, 9]). The HCN-to-HNC intensity ratio also provides information on the kinetic temperature of interstellar molecular clouds [10].

The presence of HCNH^+ has been confirmed in various interstellar regions, including the dense and cold dark cloud TMC-1 in the Taurus Molecular Cloud complex [11], the pre-stellar core L1544 [3], high-mass star forming regions [4] and the molecular cloud Sgr B2, where its rotational transitions have been originally detected [12].

Due to its astrophysical relevance, HCNH^+ has been the subject of numerous experimental and theoretical studies. In the laboratory, this ion has been characterized through rotationally resolved infrared spectroscopy and further studied across a wide spectral range, from microwave [13] to sub-millimeter wavelengths [14, 15, 16]. Fundamental vibrational bands of HCNH^+ have been previously observed: ν_1 (NH stretch) [17], ν_2 (CH stretch) [18], ν_3 (CN stretch) [19, 20], ν_4 (HCN bend) [21] and ν_5 (HNC bend) [22]. Additionally, the $\nu_1 + \nu_4 \leftarrow \nu_4$ and $\nu_1 + \nu_5 \leftarrow \nu_5$ hot bands were also explored [23]. Alongside the experiments, several theoretical studies [24, 25, 26, 27, 28] were focused on the

determination of the structure and spectroscopic properties of HCNH^+ ions.

Experimentally determined frequencies of transitions involving excitation of multiple vibrational quanta reveal information about the molecule's potential energy surface (PES) and as such are very useful to benchmark *ab initio* calculations. To our best knowledge, the overtone transitions of HCNH^+ ions have not yet been experimentally studied. This paper reports the observation of the rotationally resolved $2\nu_1$ and $2\nu_2$ overtone and $\nu_1 + \nu_2$ and $\nu_2 + \nu_3 + 2\nu_5^0$ combination bands of the HCNH^+ ion.

2. Material and Methods

2.1. Experimental

The experimental setup, Cold CAS Ion Trap – a cryogenic 22 pole radio frequency (rf) trap, has been extensively described previously [29] and only a short description will follow. The ion of interest, HCNH^+ , was produced in an ion storage source using electron bombardment in a mixture of HCN, He, and H_2 . The ion beam exiting the source is mass selected using a quadrupole mass filter and injected into a 22 pole ion trap mounted on top of a closed cycle helium cryostat. Variable temperature is achieved using a resistive heater. A short and intense helium pulse is used to trap and cool the injected ions close to the temperature of the trap walls. After a storage time of several seconds (typically 2.5 s), the trap is emptied towards a product quadrupole mass filter and the ions are counted in a Daly type detector. Laser light was delivered by an Agilent 8164B option 200 light system (1440 – 1640 nm, line width < 100 kHz, and, power 1 – 8 mW (wavelength dependent)). The wavelength was measured by an EXFO WA 1650 wavemeter with an absolute accuracy better than 0.3 ppm at 1500 nm. The scanning has only been performed in the vicinity of selected transitions and the scanning window got progressively narrower as the fit precision increased with the number of detected lines for each band. Two kodial glass windows aligned with the

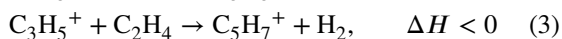
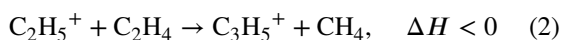
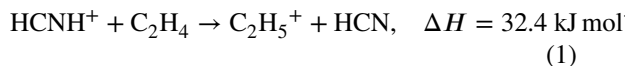
*Corresponding author

✉ pjusko@mpe.mpg.de (P. Jusko)

ORCID(s):

trap axis enabled us to use a triple pass laser beam path configuration [30].

In the present experiments, a variation of a laser induced reaction (LIR) technique [31] (an action spectroscopy scheme), was applied in order to obtain overtone spectra of HCNH^+ ions. The LIR technique takes advantage of a different reactivity of the ground and excited states of the ion of interest. For this purpose, reactant gas C_2H_4 , ethylene, has been continuously leaked into the trap (effective number density in the trap in the 10^{11} cm^{-3} range) at $T = 125 \text{ K}$ to avoid excessive freezing and the following reactions took place:



where the endothermicity of reaction (1) was calculated from the experimental proton affinities taken from the NIST database [32]. Reaction (1) is the only endothermic reaction in this system and the exothermic reactions (2–3) proceed with close to Langevin collisional reaction rate, as has been tested in a preparatory experiment, where C_2H_5^+ has been injected into the trap directly. The final product in this reaction scheme, C_5H_7^+ , reacts only very slowly with C_2H_4 , and is thus monitored as a proxy for the HCNH^+ photon excitation. We will further refer to this process as a “multi-step LIR” scheme. Moreover, as the m/z of the ion of interest HCNH^+ ($28 m/z$) is more than two times lower than that of the monitored ion C_5H_7^+ ($67 m/z$), we also applied the zero background “kick-out” technique [30], where the higher m/z product ions contributing to the background are removed from the trap by lowering the rf amplitude for few hundred milliseconds, shortly before the irradiation of HCNH^+ takes place. This ensures that all the C_5H_7^+ product ions are formed throughout the irradiation time from the LIR scheme (1)–(3).

2.2. Computational

The anharmonic vibrational frequencies computed in this study were determined using the vibrational configuration interaction theory (VCI) [33, 34, 35] implemented in the MOLPRO package of ab initio programs [36]. First, the equilibrium geometry of HCNH^+ has been determined using explicitly correlated coupled-cluster theory including single and double excitations and a perturbative treatment of the triple excitations [37] with an augmented correlation-consistent basis set [38] with the core electrons being also correlated [39], CCSD(T)-F12b/cc-pCVQZ-F12. Second, a harmonic frequency calculation was carried out in order to determine displacement vectors, which were used to span the multidimensional PES with the equilibrium geometry serving as the reference point for the expansion.

Next, an n -mode expansion [40] being truncated after the 4-mode coupling terms was utilized to generate the PES. A multilevel scheme was used [35], where the first and second

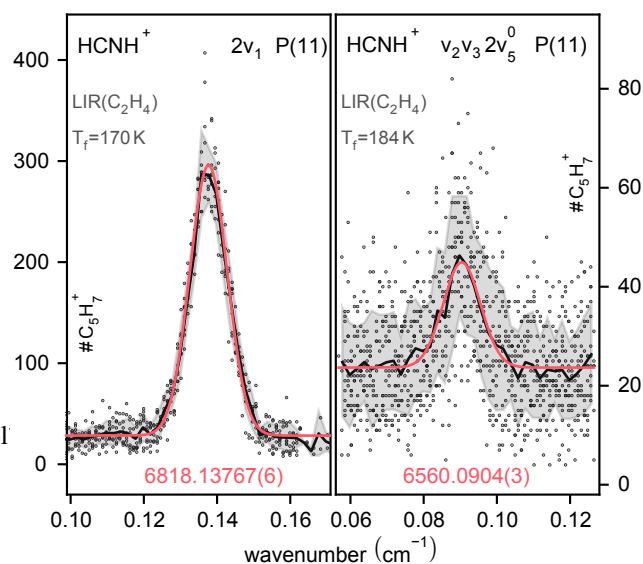


Figure 1: Measured absorption line profiles for P(11) transitions belonging to the $2\nu_1$ (left panel) and $\nu_2 + \nu_3 + 2\nu_5^0$ (right panel) vibrational bands of HCNH^+ ions. The abscissa is offset by 6818 cm^{-1} (left panel) and 6560 cm^{-1} (right panel). The temperatures T_f listed in the figure were obtained from the Doppler broadening of the absorption lines. Nominal trap temperature was 128 K .

order terms were computed at the level indicated above, while a smaller basis set, cc-pCVTZ-F12, was used for the 3rd and 4th order terms. The PES was then transformed from a grid representation to an analytical representation [41]. Using the n -mode polynomial PES, one-mode wavefunctions (modals) were determined first by vibrational self-consistent field (VSCF) [42]. These modals served as basis functions for the following VCI calculations. Vibrational states were computed up to 4 quanta excitations below 10000 cm^{-1} . The VCI configuration space converged with the maximum number of simultaneously excited modes of seven, the maximal excitation level per mode of twelve, and the maximal sum of quantum numbers of 15. The VCI convergence errors were below 0.1 cm^{-1} , while the final size of the VCI matrix was 170,488.

3. Results and Discussion

Two selected absorption lines profiles of the HCNH^+ ion acquired using the multi-step LIR scheme are shown in Figure 1. The frequency dependent numbers of trapped C_5H_7^+ ions, mimicking the absorption in the HCNH^+ ion, were fitted by a Doppler profile. The resulting center transition wavenumbers are summarised in Table A.1. To describe the upper and lower energy levels of HCNH^+ we used a standard Hamiltonian for a linear molecule [30]:

$$H = T_v + B_v J(J+1) - D_v [J(J+1)]^2 + H_v [J(J+1)]^3, \quad (4)$$

where ν represents vibrational quantum numbers of a given state, T_v , B_v , D_v and H_v are spectroscopic constants and J is the rotational quantum number. As all the probed

Table 1

Spectroscopic constants of the upper levels of the vibrational bands of HCNH^+ probed in the present study. T_{calc} denotes the predicted vibrational band origins and I_{calc} the calculated infrared intensities.

Band	I_{calc} ($\text{km} \cdot \text{mol}^{-1}$)	T_{calc} (cm^{-1})	T_v (cm^{-1})	B_v (cm^{-1})	D_v (10^{-6} cm^{-1})	H_v (10^{-9} cm^{-1})
$2\nu_1$	1.92	6851.15	6846.77981(90)	1.222953(37)	3.34(42)	2.9(1.3)
$\nu_1 + \nu_2$	1.98	6646.76	6640.47624(43)	1.221567(13)	1.698(72)	
$2\nu_2$	0.44	6284.64	6282.03578(63)	1.220617(34)	1.08(39)	
$\nu_2 + \nu_3 + 2\nu_5^0$	0.06	6608.61	6588.4894(20)	1.225412(62)	5.21(43)	

Note: Numbers in parentheses denote the statistical error of the fitted parameters in the units of the last quoted digit. T_{calc} and I_{calc} were computed with a hybrid VCI calculation at the AE-CCSD(T)/cc-pCVQZ-F12//AE-CCSD(T)/cc-pCVTZ-F12 level of theory. For details see section 2.2.

vibrational bands originated in the vibrational ground state, T_v corresponds to the band origin. The measured transition wavenumbers were fitted using Hamiltonian (4) while the spectroscopic constants for the lower state were fixed at the values recently reported by Silva et al. [16]. The obtained spectroscopic constants for the measured overtone and combination bands of HCNH^+ are listed in Table 1 together with the present theoretical predictions for the band origins (T_{calc}) and infrared intensities (I_{calc}). For the three strongest bands, T_{calc} is within 7 cm^{-1} of the experimentally determined values.

A weak band was observed close to the $\nu_1 + \nu_2$ combination band. Based on the calculated band origins and vibrational transition moments, as described in section 2.2, we identified this band as $\nu_2 + \nu_3 + 2\nu_5^0$. Note that the value of the calculated band origin for this band is 20 cm^{-1} higher than the experimental one. However, there are no other states within $\pm 150 \text{ cm}^{-1}$ apart from the transition to $\nu_2 + \nu_3 + 2\nu_5^2$ at 6621.21 cm^{-1} , which is not allowed due to the selection rules ($\Delta l = 0, \pm 1$ for a linear molecule). It is very challenging to infer absolute transition intensities from action spectroscopy spectra [30], and even relative values have to be taken with caution as the overlap between the ion cloud in the trap and the laser beam can change during experiments, especially with changing number of trapped ions (for illustration see the full line list and scattered Boltzmann plot for the $2\nu_1$ band in the data set). The two P(11) transitions for both $2\nu_1$ and $\nu_2 + \nu_3 + 2\nu_5^0$ bands depicted in Figure 1 were obtained with 22 thousand and 39 thousand of primary HCNH^+ ions, respectively. Additionally, taking into account the actual laser power, the resulting estimate for intensity ratio from the product ion signal between these two transitions is 25:1. This is in very good agreement with the calculated ratio of 31:1 (see Table 1 and section 2.2 for details) and showcases the very high sensitivity of the “kick-out” LIR technique. The strongest fundamental band ν_1 (NH stretch) of HCNH^+ has a calculated intensity of $482.46 \text{ km} \cdot \text{mol}^{-1}$, almost four orders of magnitude stronger, than that of the weak combination band, $0.06 \text{ km} \cdot \text{mol}^{-1}$. This intensity translates into a transition dipole moment of only $1.9 \cdot 10^{-3}$ Debye and to our knowledge it is the first detection of a transition involving simultaneous excitation

of 4 quanta in a high resolution ion trap based action spectroscopy experiment. We are aware of only one comparable ion trap experiment involving 3 quanta, the 3ν R(0) OH⁻ transition studied in [43].

Previous theoretical studies [25, 26, 28] focused on fundamental transitions or covered only the lower lying vibrational states [27]. Botschwina [24] arbitrarily corrected calculated potential energy curves to exactly reproduce the experimental band origins for ν_1 and ν_2 . The resulting predicted band origins for $2\nu_1$ (6858 cm^{-1}), $\nu_1 + \nu_2$ (6640 cm^{-1}) and $2\nu_2$ (6281 cm^{-1}) are very close to the present experimental values of $6846.77981(90) \text{ cm}^{-1}$, $6640.47624(43) \text{ cm}^{-1}$ and $6282.03578(63) \text{ cm}^{-1}$, respectively.

4. Conclusion

Band origins and upper state spectroscopic constants for four new overtone and combination bands of HCNH^+ ions were determined using a “kick-out” enhanced multi-step laser induced reaction technique in a 22 pole radio frequency ion trap. The application of zero background spectroscopy enables the observation of very weak transitions such as the $\nu_2 + \nu_3 + 2\nu_5^0$ reported in this study. The provided state-of-the-art *ab initio* calculations are in good agreement with the determined band origins, despite the fact that computing highly excited vibrational states (overtones and combination bands) with high accuracy can be much more challenging. Using these frequencies, the HCNH^+ ion can now easily be experimentally monitored in optically thin environments using cheap semiconductor distributed-feedback (DFB) diode lasers in the S, C, L telecommunication bands or in emission using spectrometers.

Declaration of Competing Interest

The authors report there are no competing interests to declare.

Data Availability

The data that support the findings of this study (raw experimental data, as well as the calculated PES) are openly available in Zenodo at [10.5281/zenodo.12794341](https://zenodo.org/doi/10.5281/zenodo.12794341), reference number 12794341.

Table A.1Experimentally measured transitions of HCNH⁺.

	$2\nu_1$		$\nu_1 + \nu_2$		$2\nu_2$		$\nu_2 + \nu_3 + 2\nu_5^0$
R(14)	6880.63603(26)	R(9)	6663.59689(6)	R(7)	6300.70083(12)	R(7)	6607.47736(39)
R(13)	6878.57219(20)	R(7)	6659.20677(7)	R(6)	6298.47618(11)	R(6)	6605.18607(25)
R(12)	6876.48002(17)	R(5)	6654.69970(6)	R(5)	6296.21932(24)	P(4)	6578.47191(37)
R(11)	6874.36157(14)	P(4)	6630.41455(7)	R(4)	6293.93282(24)	P(6)	6573.33680(39)
R(10)	6872.21087(12)	P(5)	6627.82652(5)	R(3)	6291.61514(11)	P(8)	6568.10975(33)
R(8)	6867.83104(10)	P(7)	6622.56541(9)	R(1)	6286.88797(21)	P(10)	6562.78773(27)
R(7)	6865.60037(16)	P(9)	6617.19029(20)	R(0)	6284.47692(32)	P(11)	6560.09040(32)
P(3)	6839.28406(11)	P(11)	6611.69643(12)			P(12)	6557.37146(48)
P(4)	6836.73553(10)	P(12)	6608.90821(14)				
P(5)	6834.15802(7)	P(13)	6606.09246(20)				
P(6)	6831.55345(6)	P(14)	6603.24654(10)				
P(7)	6828.92488(10)						
P(8)	6826.26870(7)						
P(9)	6823.58547(5)						
P(10)	6820.87529(5)						
P(11)	6818.13767(6)						
P(13)	6812.58447(21)						

Note: All values in units of cm⁻¹. In all cases the lower state is the vibrational ground state. Numbers in parentheses are statistical errors of the fit in units of the last quoted digit.

Acknowledgments

This work was supported by the Max Planck Society; Czech Science Foundation projects GACR 22-05935S, 23-05439S, 24-10992S. M.K. acknowledges support by Charles University project GAUK 337821 and that this article is based upon work from COST Action CA21101, supported by COST (European Cooperation in Science and Technology). J.S. has been supported by an ERC Advanced Grant (MissIons: 101020583). We thank Prof. Stephan Schlemmer (Uni. zu Köln) for lending of the Agilent laser system. We thank the reviewers for their constructive feedback.

A. Line lists of measured HCNH⁺ transitions

References

- [1] T. J. Millar, *Astrochemistry*, PSST 24 (2015) 043001. doi:10.1088/0963-0252/24/4/043001.
- [2] E. Herbst, W. Klemperer, The Formation and Depletion of Molecules in Dense Interstellar Clouds, *ApJ* 185 (1973) 505–534. doi:10.1086/152436.
- [3] D. Quénard, C. Vastel, C. Ceccarelli, P. Hily-Blant, B. Lefloch, R. Bachiller, Detection of the HC₃NH⁺ and HCNH⁺ ions in the L1544 pre-stellar core, *MNRAS* 470 (2017) 3194–3205. doi:10.1093/mnras/stx1373.
- [4] Fontani, F., Colzi, L., Redaelli, E., Sipilä, O., Caselli, P., First survey of HCNH⁺ in high-mass star-forming cloud cores, *A&A* 651 (2021) A94. doi:10.1051/0004-6361/202140655.
- [5] P. Dohnal, P. Jusko, M. Jiménez-Redondo, P. Caselli, Measurements of rate coefficients of CN⁺, HCN⁺, and HNC⁺ collisions with H₂ at cryogenic temperatures, *J. Chem. Phys.* 158 (2023) 244303. doi:10.1063/5.0153699.
- [6] J. Semaniak, B. F. Minaev, A. M. Derkach, F. Hellberg, A. Neau, S. Rosén, R. Thomas, M. Larsson, H. Danared, A. Paál, M. af Ugglas, Dissociative Recombination of HCNH⁺: Absolute Cross-Sections and Branching Ratios, *ApJS* 135 (2001) 275. doi:10.1086/321797.
- [7] J.-C. Loison, V. Wakelam, K. M. Hickson, The interstellar gas-phase chemistry of HCN and HNC, *Monthly Notices of the Royal Astronomical Society* 443 (2014) 398–410. doi:10.1093/mnras/stu1089.
- [8] Z. R. Todd, K. I. Öberg, Cometary delivery of hydrogen cyanide to the early earth, *Astrobiology* 20 (2020) 1109–1120. doi:10.1089/ast.2019.2187.
- [9] B. K. D. Pearce, K. Molaverdikhani, R. E. Pudritz, T. Henning, K. E. Cerrillo, Toward RNA life on early earth: From atmospheric hcn to biomolecule production in warm little ponds, *The Astrophysical Journal* 932 (2022) 9. doi:10.3847/1538-4357/ac47a1.
- [10] Hacar, A., Bosman, A. D., van Dishoeck, E. F., HCN-to-HNC intensity ratio: a new chemical thermometer for the molecular ism, *A&A* 635 (2020) A4. doi:10.1051/0004-6361/201936516.
- [11] L. M. Ziurys, A. J. Apponi, J. T. Yoder, Detection of the Quadrupole Hyperfine Structure in HCNH⁺, *ApJL* 397 (1992) L123. doi:10.1086/186560.
- [12] L. M. Ziurys, B. E. Turner, HCNH⁺: A New Interstellar Molecular Ion, *ApJL* 302 (1986) L31. doi:10.1086/184631.
- [13] M. Araki, H. Ozeki, S. Saito, Laboratory measurement of the pure rotational transitions of hcnh⁺ and its isotopic species, *ApJ* 496 (1998) L53. doi:10.1086/311245.
- [14] M. Bogey, C. Demuyneck, J. L. Destombes, Millimeter and submillimeter wave spectrum of HCNH⁺, *J. Chem. Phys.* 83 (1985) 3703–3705. doi:10.1063/1.449126.
- [15] T. Amano, K. Hashimoto, T. Hirao, Submillimeter-wave spectroscopy of HCNH⁺ and CH₃CNH⁺, *J. Mol. Struct.* 795 (2006) 190–193. doi:10.1016/j.molstruc.2006.02.035.
- [16] W. G. D. P. Silva, L. Bonah, P. C. Schmid, S. Schlemmer, O. Asvany, Hyperfine-resolved rotational spectroscopy of HCNH⁺, *J. Chem. Phys.* 160 (2024) 071101. doi:10.1063/5.0185365.
- [17] R. S. Altman, M. W. Crofton, T. Oka, High resolution infrared spectroscopy of the ν_1 (NH stretch) and ν_2 (CH stretch) bands of HCNH⁺, *J. Chem. Phys.* 81 (1984) 4255–4258. doi:10.1063/1.447433.
- [18] R. S. Altman, M. W. Crofton, T. Oka, Observation of the infrared ν_2 band (CH stretch) of protonated hydrogen cyanide HCNH⁺, *J. Chem. Phys.* 80 (1984) 3911–3912. doi:10.1063/1.447173.
- [19] M. Kajita, K. Kawaguchi, E. Hirota, Diode laser spectroscopy of the ν_3 (CN stretch) band of HCNH⁺, *J. Mol. Spectrosc.* 127 (1988) 275–276. doi:10.1016/0022-2852(88)90026-4.

- [20] D.-J. Liu, S.-T. Lee, T. Oka, The ν_3 fundamental band of HCNH^+ and the $2\nu_3 \leftarrow \nu_3$ and $\nu_2 + \nu_3 \leftarrow \nu_2$ hot bands of HCO^+ , *J. Mol. Spectrosc.* 128 (1988) 236–249. doi:10.1016/0022-2852(88)90221-4.
- [21] K. Tanaka, K. Kawaguchi, E. Hirota, Diode laser spectroscopy of the ν_4 (HCN bend) band of HCNH^+ , *J. Mol. Spectrosc.* 117 (1986) 408–415. doi:10.1016/0022-2852(86)90164-5.
- [22] W.-C. Ho, C. E. Blom, D.-J. Liu, T. Oka, The infrared ν_5 band (HNC bend) of protonated hydrogen cyanide, HCNH^+ , *J. Mol. Spectrosc.* 123 (1987) 251–253. doi:10.1016/0022-2852(87)90275-X.
- [23] T. Amano, K. Tanaka, Difference frequency laser spectroscopy of HCNH^+ : Observation of the isotopic species and the hot bands, *J. Mol. Spectrosc.* 116 (1986) 112–119. doi:10.1016/0022-2852(86)90257-2.
- [24] P. Botschwina, Spectroscopic properties of HCNH^+ calculated by SCEP CEPA, *Chem. Phys. Lett.* 124 (1986) 382–390. doi:10.1016/0009-2614(86)85038-2.
- [25] P. Botschwina, A. Heyl, M. Horn, J. Flugge, Calculated Spectroscopic Constants and the Equilibrium Geometry of HCNH^+ , *J. Mol. Spectrosc.* 163 (1994) 127–137. doi:10.1006/jmsp.1994.1013.
- [26] P. E. Peterson, M. Abu-Omar, T. W. Johnson, R. Parham, D. Goldin, C. I. Henry, A. Cook, K. M. Dunn, Ab initio predictions of vibrational frequencies for cationic species, *J. Phys. Chem.* 99 (1995) 5927–5933. doi:10.1021/j100016a030.
- [27] V. Brites, L. Jutier, New ab initio study of the spectroscopy of HCNH^+ , *J. Mol. Spectrosc.* 271 (2012) 25–32. doi:10.1016/j.jms.2011.11.004.
- [28] C. Eric Cotton, J. S. Francisco, W. Klemperer, Computational study of the linear proton bound ion–molecule complexes of HCNH^+ with HCN and HNC, *J. Chem. Phys.* 139 (2013) 014304. doi:10.1063/1.4811834.
- [29] P. Jusko, M. Jiménez-Redondo, P. Caselli, Cold cas ion trap – 22 pole trap with ring electrodes for astrochemistry, *Mol. Phys.* 122 (2024) e2217744. doi:10.1080/00268976.2023.2217744.
- [30] M. Jiménez-Redondo, L. Uvarova, P. Dohnal, M. Kassayová, P. Caselli, P. Jusko, Overtone transition $2\nu_1$ of HCO^+ and HOC^+ : Origin, radiative lifetime, collisional quenching, *ChemPhysChem* 25 (2024) e202400106. doi:10.1002/cphc.202400106.
- [31] S. Schlemmer, T. Kuhn, E. Lescop, D. Gerlich, Laser excited N_2^+ in a 22-pole ion trap:: Experimental studies of rotational relaxation processes, *Int. J. Mass Spectrom.* 185-187 (1999) 589–602. doi:10.1016/S1387-3806(98)14141-6.
- [32] P. J. Lindstrom, W. G. Mallard, NIST Chemistry WebBook, NIST Standard Reference Database Number 69, NIST, Gaithersburg MD, 20899, 2023. doi:10.18434/T4D303.
- [33] T. Mathea, G. Rauhut, Advances in vibrational configuration interaction theory - part 1: Efficient calculation of vibrational angular momentum terms., *J. Comput. Chem.* 42 (2021) 2321–2333. doi:10.1002/jcc.26762.
- [34] T. Mathea, T. Petrenko, G. Rauhut, Advances in vibrational configuration interaction theory - part 2: Fast screening of the correlation space., *J. Comput. Chem.* 43 (2022) 6–18. doi:10.1002/jcc.26764.
- [35] B. Schröder, G. Rauhut, From the automated calculation of potential energy surfaces to accurate vibrational spectra, *J. Phys. Chem. Lett.* 15 (2024) 3159. doi:10.1021/acs.jpcl.4c00186.
- [36] H. J. Werner, P. J. Knowles, F. R. Manby, J. A. Black, K. Doll, A. Heßelmann, D. Kats, A. Köhn, T. Korona, D. A. Kreplin, Q. Ma, T. F. Miller, A. Mitrushchenkov, K. A. Peterson, I. Polyak, G. Rauhut, M. Sibaev, The molpro quantum chemistry package, *J. Chem. Phys.* 152 (2020) 144107. doi:10.1063/5.0005081.
- [37] T. B. Adler, G. Knizia, H.-J. Werner, A simple and efficient CCSD(T)-F12 approximation, *J. Chem. Phys.* 127 (2007) 221106. doi:10.1063/1.2817618.
- [38] K. A. Peterson, T. B. Adler, H.-J. Werner, Systematically convergent basis sets for explicitly correlated wavefunctions: The atoms H, He, B–Ne, and Al–Ar, *J. Chem. Phys.* 128 (2008) 084102. doi:10.1063/1.2831537.
- [39] J. G. Hill, S. Mazumder, K. A. Peterson, Correlation consistent basis sets for molecular core-valence effects with explicitly correlated wave functions: The atoms B–Ne and Al–Ar, *J. Chem. Phys.* 132 (2010) 054108. doi:10.1063/1.3308483.
- [40] J. M. Bowman, T. C. Jr., H. D. Meyer, Variational quantum approaches for computing vibrational energies of polyatomic molecules, *Mol. Phys.* 106 (2008) 2145. doi:10.1080/00268970802258609.
- [41] B. Ziegler, G. Rauhut, Efficient generation of sum-of-products representations of high-dimensional potential energy surfaces based on multimode expansions, *J. Chem. Phys.* 144 (2016) 114114. doi:10.1063/1.4943985.
- [42] J. Meisner, P. Hallmen, J. Kästner, G. Rauhut, Vibrational analysis of methyl cation - rare gas atom complexes: CH_3^+ -Rg (Rg=He, Ne, Ar, Kr), *J. Chem. Phys.* 150 (2019) 084306. doi:10.1063/1.5084100.
- [43] O. Lakhmanskaya, M. Simpson, R. Wester, Vibrational overtone spectroscopy of cold trapped hydroxyl anions, *Phys. Rev. A* 102 (2020) 012809. doi:10.1103/PhysRevA.102.012809.